

## Event rates of UHE photons cascading in the geomagnetic field at CTA-North

**Kevin Almeida Cheminant<sup>a,\*</sup> and Dariusz Góra<sup>a</sup> on behalf of the CREDO Collaboration**

(a complete list of authors can be found at the end of the proceedings)

<sup>a</sup>*Institute of Nuclear Physics Polish Academy of Sciences,  
Radzikowskiego 152, 31-342 Krakow, Poland*

*E-mail:* [kevin.almeida-cheminant@ifj.edu.pl](mailto:kevin.almeida-cheminant@ifj.edu.pl), [dariusz.gora@ifj.edu.pl](mailto:dariusz.gora@ifj.edu.pl)

Photons in the EeV range and beyond are expected from top-down models of UHECR production and from the GZK effect. As they reach the Earth, they have a non-zero probability of converting into an electron/positron pair in the geomagnetic field and of producing an electromagnetic shower above the atmosphere. In this work, we present a new method to search for cascading UHE photons with gamma-ray telescopes based on Monte-Carlo simulations and multivariate analyses. Considering the future CTA-North experiment in La Palma, Spain, we show that such a method provides an efficient cosmic-ray background rejection with little loss of cascading UHE photon events. We also estimate that if gamma-ray bursts photon emission extends to the EeV regime, the number of expected events in 30 hours of observation time can go up to 0.17.

*37<sup>th</sup> International Cosmic Ray Conference (ICRC 2021)  
July 12th – 23rd, 2021  
Online – Berlin, Germany*

---

\*Presenter

## 1. Introduction

In astroparticle physics, several theoretical models predict the production of ultra-high energy (UHE) photons (EeV and beyond), that would constitute a fraction of the ultra-high energy cosmic-ray (UHECR) flux seen on Earth. Whether they emerge as the result of the interaction of UHE protons or nuclei with the cosmic microwave background (CMB) [1, 2], or from the decay of supermassive particles [3–5], the direction of propagation of UHE photons is unaffected by electromagnetic fields, which makes them valuable messengers in the identification of sources of UHECRs. Nevertheless, the highest energy events observed by the leading collaborations, the Pierre Auger Observatory (Auger) [6] and Telescope Array (TA) [7], are not considered photon candidates, if the present state-of-the-art air-shower reconstruction procedures are applied.

The most straightforward explanation for the absence of UHE photon observations could simply be related to the absence of physical mechanisms responsible for their production, therefore refuting predictions made by both classical bottom-up and exotic top-down scenarios of UHECR production. Although rather simplistic and quite effortless, such an explanation remains fully conceivable, as recent experimental limits from Auger and TA on the UHE photon flux strongly disfavor the exotic models [8, 9]. Alternatively, as predicted by Lorentz invariance violation models, UHE photons may decay after a very short period of time (of the order of 1 second) [10, 11]. In this case, their decay occurs nearly immediately after their production and gives them no chance to reach the Earth, making direct observations of such photons almost impossible. One can also speculate that UHE photons do not reach the Earth because of some yet unknown, or not well-understood, processes occurring before entering the Earth’s atmosphere. As these photons travel through space, they may interact with electromagnetic fields of different origin and produce cascades of secondary particles of lower energy. Such screening effect leads to the production of air showers, whose properties may differ from the ones of unconverted photons.

In order to increase the chance probability of detecting UHE photons, we propose to include ground Imaging Atmospheric Cherenkov Telescopes (IACTs) in their search [12]. Due to the low expected flux of particles in the UHE domain and to the energy threshold of IACTs, the standard vertical mode of observation of gamma-ray telescopes is no longer efficient. The use of gamma-ray telescopes in a non-standard approach, i.e. in the nearly-horizontal direction, is therefore considered [13]. Looking at nearly-horizontal air showers makes possible the isolation of the muonic component, which constitutes a great discriminator to identify EASs’ primaries. Furthermore, looking for air showers at high zenith angles offers a greater collection area, about 10-100 times larger, compared to the typical aperture of gamma-ray experiments in the standard mode of observation. However, due to the geometry of the cascade development, the Cherenkov light detected by the IACT cameras is produced further away from the telescopes. In the TeV domain, such a characteristic leads to the formation of very small images in the cameras, often within a single pixel, and therefore results in a poor photon/hadron separation. However, in the EeV domain, the dominating muonic component can produce brighter and larger images such that a good separation can be recovered.

UHE photons propagating through strong magnetic fields have a probability of converting into a pair of  $e^-/e^+$  close to 1 when reaching the Earth at high zenith angles. When such a conversion occurs in the Earth’s magnetic field, this phenomenon is referred to as *preshower* effect

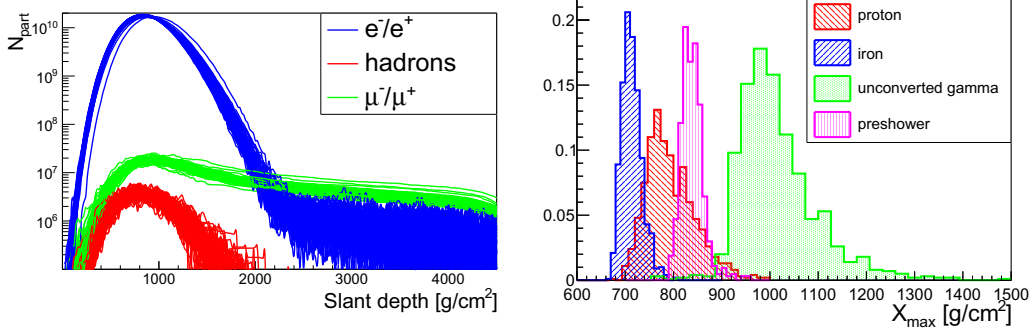


**Figure 1:** *Left:* Longitudinal profiles of electrons, hadrons and muons of 10 nearly-horizontal EAS's produced by 40 EeV photons affected by the preshower effect. *Right:*  $X_{max}$  distribution of the nearly-horizontal EASs initiated by 40 EeV primaries. NOTE: the location of the CTA-North site at 2200 m is equivalent to a slant depth of 4550 g/cm<sup>2</sup> at 80° zenith angle.

[14]. In this study, the feasibility of observing very inclined air showers produced by this effect was investigated through Monte-Carlo simulations, taking the example of the next generation of gamma-ray telescopes developed by the CTA collaboration, with a special attention given to CTA-North, which is planned to be located in La Palma, Canary Islands [15]. The images formed in CTA-North cameras by the cosmic-ray (CR) background and preshower-induced air showers are analyzed and compared, through a set of geometrical parameters that characterize these images. With a multivariate analysis, the CR background/converted UHE photon separation power obtained assuming properties of the CTA-North design, and for point sources of UHE photons, was investigated. From the results of the multivariate analysis, the number of events that should be detected based on the upper limits on the UHE photon flux from point sources set by Auger [16] and TA [17] and by the extrapolation of gamma-ray emission from gamma-ray bursts (GRB) at the highest energies, was estimated.

## 2. Preshower/CR Background simulations

The study of the properties of preshowers was carried out by investigating different energies for the primary photons, as well as different arrival directions, with a particular attention given to the case where photons are headed towards La Palma. To do so, the PRESOWER algorithm was used [18]. For a given azimuth angle, the probability increases with the energy and is null for photons with energy of a few EeV [12]. The azimuth angle for which the maximum conversion probability is reached, depends on the location of the observation site. For La Palma, which is on the northern hemisphere, the peak is observed in the direction of the geomagnetic North, which can be explained by the fact that the magnetic field is stronger close to the pole, therefore increasing the chance of UHE photons to produce pairs of  $e^-/e^+$ . The  $e^+/e^-$  pairs lose energy predominantly through the emission of bremsstrahlung photons of lower energy and the negligible deflection of the pair by the geomagnetic field leads to a large number of electromagnetic particles contained within an area of a few cm<sup>2</sup>. In the subsequent part of this work, we focus on 40 EeV photons coming at 80° zenith angle and 180° azimuth angle.

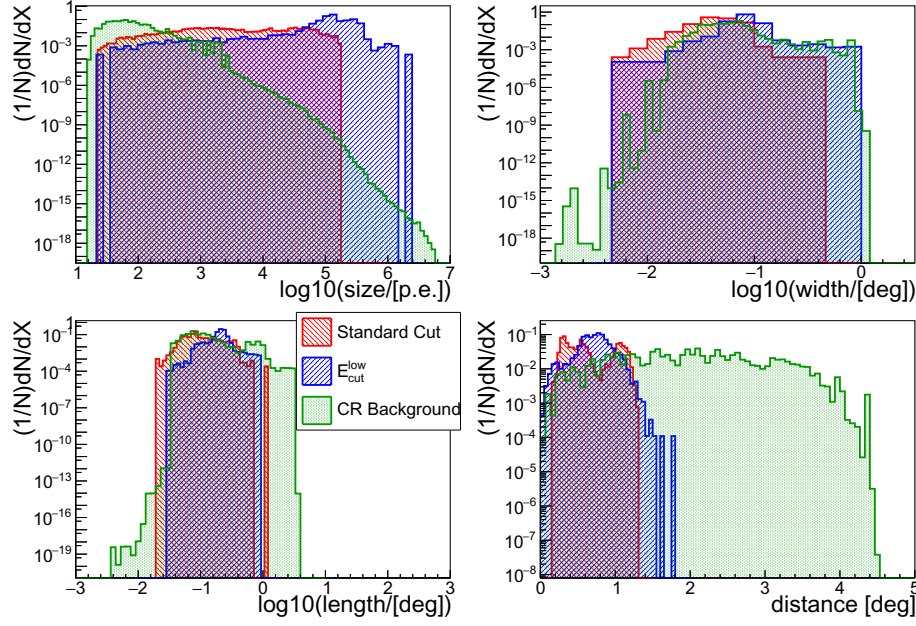


**Figure 2:** Normalized Hillas distributions for point sources of preshower with standard energy cuts used in the BDT analysis (red) and with lower energy cuts described in the *Outlook* section. CR background distributions are also shown in green.

When these preshowers reach the atmosphere, they may in turn initiate extensive air showers (EASs). The properties of these showers, such as their composition, their longitudinal development, their ground distribution, and the origin of the Cherenkov light they emit, can be examined via the CORSIKA simulation software [19]<sup>1</sup>. Figure 1 (left) shows the evolution of the air showers components as a function of the depth of the atmosphere for a preshower initiated by a 40 EeV photon. Around 2300 g/cm<sup>2</sup>, the muonic component dominates the further stages of the shower development. Figure 1 (right) shows where EASs initiated by different primaries with an energy of 40 EeV reach their maximum development  $X_{\max}$ . The preshower effect tends to produce EASs that reach their maximum higher up in the atmosphere, closer to where hadronic showers reach theirs, as the first interaction point can occur thousands of kilometers above the atmosphere. Such property makes EASs from "preshowered" photons more similar to hadronic ones, such that experiments relying solely on  $X_{\max}$  measurements may misinterpret the primary identification if such an effect is not taken into account. In order to reduce the computing time of preshower simulations used in the multivariate analysis, we used high energy cuts (6000, 4000, 500 and 500 GeV for hadrons, muons, electrons and gammas, respectively) and of the thinning algorithm of CORSIKA. The maximum impact distance of the EASs core was also randomized within a circle of radius 1300 m centered around the direction defined in the previous paragraph. The CR background was simulated in 13 energy bins for a pure proton composition between 10 TeV and 10 EeV according to the CR spectrum, with a direction randomized within a cone of 5° opening.

The Cherenkov light emitted by EASs can be recorded by the cameras of IACTs in the form of images generated by triggered pixels. The main focus is set on simulating the cameras

<sup>1</sup>See reference [12] for more details regarding the hadronic models used and the options activated in CORSIKA.

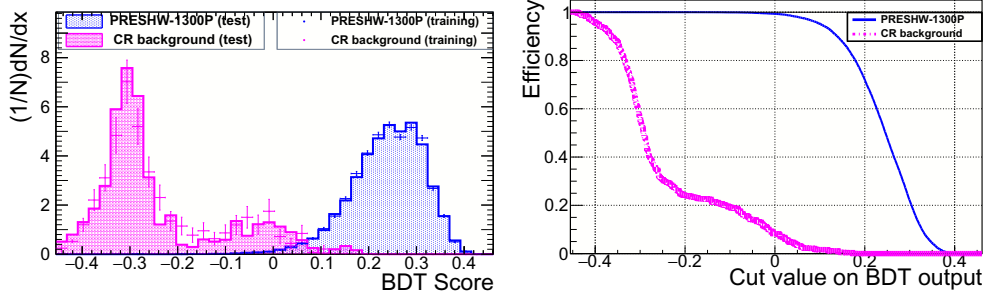


**Figure 3:** Left: BDT score of point sources of preshowers and of the CR background. Both training and testing distributions are shown. Right: Efficiency as a function of the cut on the BDT score distributions.

properties and the geographical location of CTA-North with the *sim\_telarray* package [20]. The trigger conditions are set to a minimum of 2 triggered telescopes with 3 triggered pixels. The images produced by the Cherenkov light can be characterized by a set of geometrical parameters, called Hillas parameters [21], which can be used to discriminate between images formed by the CR background and by preshowers. As shown in Figure 2, tend to be smaller (*length* and *width* distributions) and dimmer (*size* distributions), due to the significantly larger number of muons found in hadronic showers at ultra-high energy. The *distance* parameter, which characterizes the angular distance between the center of the camera and the source position, is expected to be larger if the shower axis is not aligned with the pointing direction of the telescopes, as it is the case with isotropic CR-initiated EASs.

The full simulation chain has provided almost 40 000 images of preshowers and 240 000 for the CR background. The Hillas parameters of these images were fed into a Boosted Decision Trees (BDT) analysis provided by the TMVA package [22] in order to evaluate the efficiency with which the CR background can be rejected. Half of the images were used to train 800 trees while the other half was used to test the trained classifier<sup>2</sup>. Each image, signal or background, is assigned with a score. The BDT score distributions are shown in the left panel of Figure 3. Appropriate cuts on these distributions can provide observations with very small background contamination, as the efficiency plot in the right panel of Figure 3 shows.

### 3. UHE photon event rates from GRBs

Using these results, the aperture and the number of expected preshowers can be calculated for different upper limits set by Auger and TA on point sources of UHE photons. The aperture is defined as a function of the area within which showers are simulated ( $\pi R_{\text{max}}^2$ ) and of the number of events that actually trigger the telescope array, as shown in Figure 4. For the parameters used in our simulations, we found an aperture of approximately 3.42 km<sup>2</sup> for point sources of preshowers.

Furthermore, knowing the aperture allows us to estimate the number of preshowers one could expect to observe in a given amount of time. This number can be written as:

$$N_{\text{preshw}}(E) = \phi_{\gamma}(40 \text{ EeV}) \epsilon_{\text{conv}} \Delta t A_{\text{eff}}, \quad (1)$$

<sup>2</sup>See reference [12] for more details regarding the hyperparameters of the method.

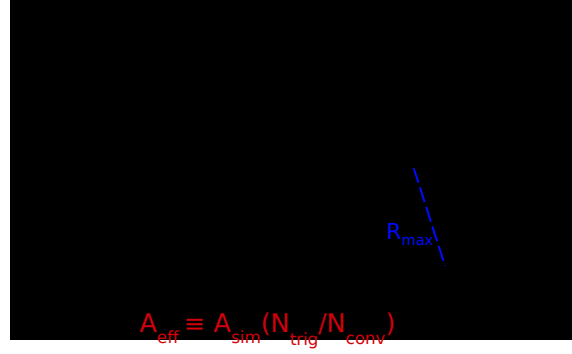


**Figure 4:** Definition of the effective area – relation between the number of preshower events simulated  $N_{\text{conv}}$  in a generation plane  $A_{\text{sim}}$  within which events are simulated homogeneously, and the effective area  $A_{\text{eff}}$  with  $N_{\text{trig}}$  events triggering the array.

where we set  $\Delta t$  to 30 hours and  $\epsilon_{\text{conv}} \sim 0.67$  is the fraction of UHE photons converting in the geomagnetic field for the energy and direction given previously. The  $\phi_\gamma$  (40 EeV) factor is the upper limit on UHE photon flux set by Auger on the Galactic center [16] and by TA on point source emission in the northern sky (average and local) [17]. These limits are reported in the second row of Table 1. The expected number of preshower from these limits are given in the third row. However, in the case of GRB flares, it is possible to imagine that photon flux may be boosted. Following MAGIC and H.E.S.S. observations of such flares [23, 24], we calculated the factor  $R$  by which such a boost may occur by comparing the flux measured by these two collaborations to the flux of the Galactic center without transient events [25]. In the case of H.E.S.S. afterglow observation, we found  $R = 5$ , while  $R = 652$  for MAGIC’s detection was calculated. The number of expected preshowers from such a boost is obtained by multiplying  $R$  to the upper limits, and is reported in the last two rows of Table 1. In such a scenario, one could expect to see almost up to 0.2 events in 30 hours of observation, which could be collected in consecutive observations of long-lasting flares.

#### 4. Outlook

Underestimation of the number of expected preshower events may arise from the high energy cuts used in the simulations and from the small maximum impact distance allowed. The influence of the energy cuts on the Hillas distributions is also illustrated in Figure 2. While the red histograms are the distributions from the standard cuts used, so far, in this analysis, the blue ones are obtained

	AUGER <sub>point</sub>	$\langle \text{TA}_{E>31.6 \text{ EeV}} \rangle$	$\text{max}(\text{TA}_{E>31.6 \text{ EeV}})$
$\phi_{\gamma-p.} (40 \text{ EeV}) [\text{km}^{-2}\text{yr}^{-1}]$	0.034	0.0073	0.019
$N_{\text{preshw}} - \text{non-transient} (R = 1)$	$2.7 \times 10^{-4}$	$5.7 \times 10^{-5}$	$1.5 \times 10^{-4}$
– $R = 5$	$1.4 \times 10^{-3}$	$2.9 \times 10^{-4}$	$7.6 \times 10^{-4}$
– $R = 652$	0.17	0.037	0.09

**Table 1:** Point sources of UHE photons – Number of preshowers expected in 30 hours of observation based on the limits set by Auger [16] and TA [17] as described in the text and on the boosted emission of the UHE photon flux by GRBs.

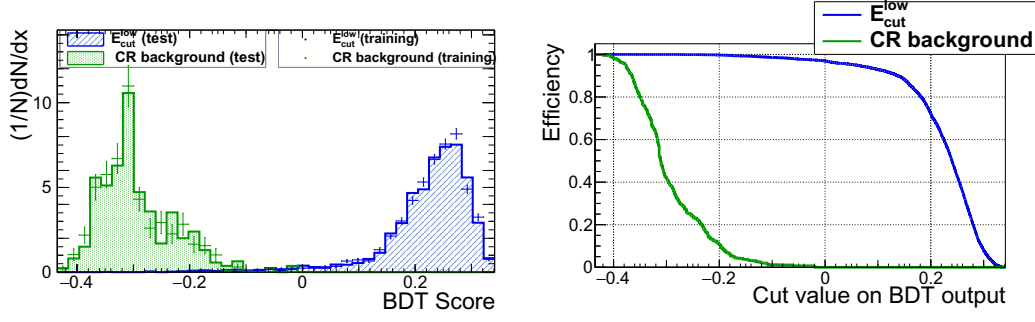


**Figure 5:** BDT score distributions of the testing and training samples (left) and efficiencies (right) of CR background and preshowers with  $R_{\text{max}} = 1300$  m and with the energy cuts described in the text.

for lower energy cuts  $E_{\text{cut}}^{\text{low}}$ , i.e. 300, 300, 3 and 3 GeV, for hadrons, muons, electrons and gammas, respectively. The Hillas distributions of the CR background used in the multivariate analysis are also shown for comparison. The lower energy cuts are essentially characterized by brighter and larger images. These two features are easily explained by the fact that charged particles of lower energies also emit Cherenkov radiation. Moreover, the larger lateral spread of these particles leads to images formed further away from the source location, resulting in higher values of the *distance* parameter.

Figure 5 shows the BDT score distributions and the efficiencies obtained for energy cuts set to  $E_{\text{cut}}^{\text{low}}$  when simulating point sources of converted UHE photons with  $R_{\text{max}} = 1300$  m. This preliminary results shows that even in this case, the photon/hadron separation remains very good and observation of preshower events in the nearly-horizontal direction could still be performed at high signal efficiencies and low background contamination.

The size of the collection area on the ground for 40 EeV converted photons in the nearly-horizontal direction is significantly larger than in the standard mode of observation. Figure 6 shows the size of the area for which preshower events, represented by red dots, have triggered the telescopes of CTA-North, for  $R_{\text{max}} = 8$  and 20 km. For  $R_{\text{max}} = 20$  km, the size of the area is  $\sim 1450$  km<sup>2</sup>, and does not increase significantly for larger  $R_{\text{max}}$  values. If an efficiency of 1 is considered, such collection area results in an optimal aperture of  $\sim 250$  km<sup>2</sup> at zenith angle  $\theta = 80^\circ$ . One can note the growing asymmetry of the collection area when compared to the location of CTA-North (black dot), as more events with the shower core hitting in front of the telescopes, trigger the array.

A new method for observation of UHE photons in the EeV domain, consisting in searching for preshower cascades in the nearly-horizontal direction, was presented in this work [12]. Such a strategy could already be applied to other experiments, such as MAGIC, which already contains data in the observation mode discussed in this work, in the Crab Nebula vicinity.

## Acknowledgments

This research has been supported in part by PLGrid Infrastructure. We warmly thank the staff at ACC Cyfronet AGH-UST, for their always helpful supercomputing support. We also want to acknowledge the support from National Science Centre in Poland, grant No. 2020/39/B/ST9/01398.



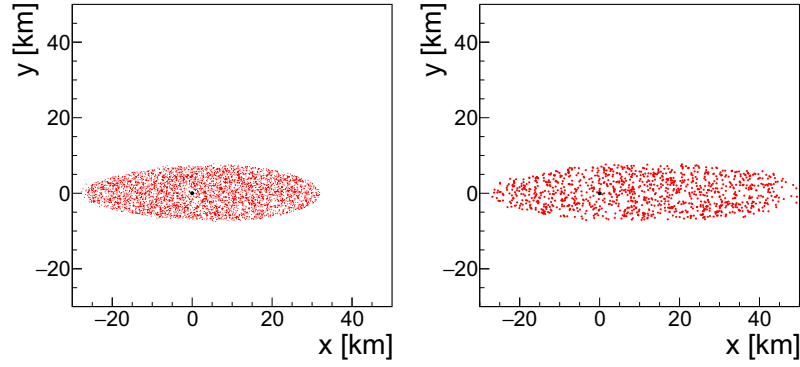


**Figure 6:** Location of impact points (red dots) of EASs produced by converted UHE photons that have triggered the array located at (0,0) which is represented by a black disk, for different maximal impact distances  $R_{\max} = 8$  km (left) and 20 km (right).

## References

- [1] K. Greisen. *Phys. Rev. Lett.*, 16:748, 1966.
- [2] G.T. Zatsepin and V.A. Kuzmin. *JETP Lett.*, 4:78, 1966.
- [3] D.J.H. Chung et al. *Phys. Rev. D*, 59(2):023501, 1998.
- [4] V.A. Kuzmin et al. *JETP Letters*, 68(4):271, 1998.
- [5] V. Berezhinsky. *Nucl. Phys. B*, 81:311, 2000.
- [6] Pierre Auger Collaboration. *Astropart. Phys.*, 34(5):314, 2010.
- [7] Telescope Array Collaboration. *The Astrophysical Journal Letters*, 790(2):L21, 2014.
- [8] Pierre Auger and the Telescope Array Collaborations. *Proc. of 36th ICRC*, 398, 2019.
- [9] Telescope Array Collaboration. *Astropart. Phys.*, 110:8, 2019.
- [10] L. Maccione, S. Liberati, and G. Sigl. *Phys. Rev. Lett.*, 105:021101, 2010.
- [11] S. Liberati and L. Maccione. *Ann. Rev. Nucl. Part. Sci.*, 59:245, 2009.
- [12] CREDO Collaboration. *Astropart. Phys.*, 123:102489, 2020.
- [13] A. Neronov et al. *Phys. Rev. D*, 94:123018, 2016.
- [14] B. McBreen and C.J. Lambert. *Phys. Rev. D*, 24(9):2536, 1981.
- [15] CTA Collaboration. *Science with the Cherenkov Telescope Array*. World Scientific, 2019.
- [16] Pierre Auger Collaboration. *Astrophys. J. Lett.*, 837(2):L25, 2017.
- [17] Telescope Array Collaboration. *Mon. Not. R. Astron. Soc.*, 492(3):3984, 2020.
- [18] P. Homola et al. *Comput. Phys. Commun.*, 173(1-2):71, 2005.
- [19] D. Heck et al. *FZKA Report*, 6019: , 1998.
- [20] K. Bernlöhner. *Astropart. Phys.*, 30:149, 2008.
- [21] A.M. Hillas. *Proceedings of 19th ICRC*, 3:445, 1985.
- [22] Andreas Hoecker, Peter Speckmayer, Joerg Stelzer, Jan Therhaag, Eckhard von Toerne, and Helge Voss. TMVA: Toolkit for Multivariate Data Analysis. *PoS, ACAT:040*, 2007.
- [23] H. Abdalla, R. Adam, F. Aharonian et al. *Nature*, 575:464, 2019.
- [24] V.A. Acciari, S. Ansoldi, L.A. Antonelli et al. *Nature*, 575:455, 2019.
- [25] A. Abramowski, F. Aharonian, F. Benkhali et al. *Nature*, 531:476, 2016.



**Full Authors List: CREDO Collaboration**

Kevin Almeida Cheminant<sup>1</sup>, Dariusz Góra<sup>1</sup>, David E. Alvarez Castillo<sup>1,2</sup>, Nikolay Budnev<sup>3</sup>, Alok C. Gupta<sup>4</sup>, Piotr Homola<sup>1</sup>, Bartosz Łozowski<sup>5</sup>, Mikhail V. Medvedev<sup>6,7</sup>, Alona Mozgova<sup>8</sup>, Maciej Pawlik<sup>9,10</sup>, Krzysztof Rzecki<sup>10</sup>, Karel Smolek<sup>11</sup>, Jarosław Stasielak<sup>1</sup>, Oleksandr Sushchov<sup>1</sup>, Arman Tursunov<sup>12</sup>, Tadeusz Wibig<sup>13</sup>, Jilberto Zamora-Saa<sup>14</sup>.

<sup>1</sup>Institute of Nuclear Physics Polish Academy of Sciences, Radzikowskiego 152, 31-342 Krakow, Poland.

<sup>2</sup>Joint Institute for Nuclear Research, Dubna, 141980 Russia.

<sup>3</sup>Irkutsk State University, Karl Marx 1, Irkutsk, 664003 Russia.

<sup>4</sup>Aryabhata Research Institute of Observational Sciences (ARIES), Manora Peak, Nainital 263001, India.

<sup>5</sup>Faculty of Natural Sciences, University of Silesia in Katowice, Bankowa 9, 40-007 Katowice, Poland.

<sup>6</sup>Department of Physics and Astronomy, University of Kansas, Lawrence, KS 66045, USA.

<sup>7</sup>Laboratory for Nuclear Science, Massachusetts Institute of Technology, Cambridge, MA 02139, USA.

<sup>8</sup>Astronomical Observatory of Taras Shevchenko National University of Kyiv, 04053 Kyiv, Ukraine.

<sup>9</sup>ACC Cyfronet AGH-UST, 30-950 Kraków, Poland.

<sup>10</sup>AGH University of Science and Technology, 30-059 Krakow, Poland.

<sup>11</sup>Institute of Experimental and Applied Physics, Czech Technical University in Prague, Husova 240/5, 110 00 Prague, Czech Republic.

<sup>12</sup>Research Centre for Theoretical Physics and Astrophysics, Institute of Physics, Silesian University in Opava, Bezručovo nám. 13, CZ-74601 Opava, Czech Republic.

<sup>13</sup>University of Łódź, Faculty of Physics and Applied Informatics, Łódź, Poland.

<sup>14</sup>Departamento de Ciencias Físicas, Universidad Andres Bello, Piso 7, Sazie 2212, Santiago, Chile.